

An intelligent Lane-Changing Behavior Prediction and Decision-Making strategy for an Autonomous Vehicle

Weida Wang, Tianqi Qie, Chao Yang, *Member, IEEE*, Wenjie Liu, Changle Xiang, and Kun Huang

Abstract—In the future complex intelligent transportation environments, lane-changing behavior of surrounding vehicles is a significant factor affecting the driving safety. It is necessary to predict the lane-changing behaviors accurately. The driving environments and drivers are the main factors of lane-changing. To comprehensively consider their relationship, this paper proposes a prediction method based on a fuzzy inference system (FIS) and a long short-term memory (LSTM) neural network. Firstly, to highly integrate driving environments with drivers, drivers' cognitive processes of driving environments are simulated using FIS. Fuzzy rules are formulated based on drivers' cognition, and then driving environments information can be transformed into lane-changing feasibility. Secondly, the obtained lane-changing feasibility and corresponding vehicle trajectory are designed as input variables of LSTM neural network to predict the lane-changing behavior. Thirdly, based on the above prediction results, an intelligent decision-making strategy is designed for path planning of autonomous vehicle to ensure driving safety. The prediction method is trained and tested by the NGSIM dataset, which is made up of real vehicle trajectories. The accurate rate of the method is 92.40%. Moreover, the decision strategy is simulated and verified in hardware in the loop system. Results show that the strategy can significantly improve the performance of driving in dealing with lane changing behaviors.

Index Terms—Lane-changing behavior prediction, autonomous vehicle, decision-making, fuzzy inference system, long short-term memory.

I. INTRODUCTION

Recently, autonomous vehicles have attracted considerable attention because of their promising benefits in improving safety and efficiency [1]. In some limited situations, autonomous vehicles have been tested and performed well at present. Obviously, it is still difficult to be widely applied in complex environments [2]. One of the reasons is the uncertain lane-changing behaviors around autonomous vehicles, which is a crucial problem for driving safety [3]. To solving the problem, lane-changing behaviors should be predicted in complex environments. Through the prediction, autonomous vehicles can adjust their motions in advance to keep a safe distance from threatening lane-changing vehicles. However, the driving environments are complex and the drivers' driving styles are uncertain. Due to the random variety of drivers' styles and the influence of the driving environments, it is difficult to predict

the motions of vehicles [4]. Therefore, how to improve the prediction accuracy has become a hotspot in the research area of autonomous vehicles.

For the above issue, many researchers have done a lot of studies and made significant progress. These studies can be divided into two categories. One is the prediction of vehicle lane-changing trajectories, and the other is the prediction of vehicle lane-changing behaviors. For lane-changing trajectories prediction, physics-based methods are proposed, which can reflect the dynamic and kinematic characteristics of vehicles to predict their future motions [5]. Generally, due to a large number of vehicle maneuvers, a single model is difficult to represent all the possible maneuvers [6]. To overcome this limitation, an interactive multiple models (IMM)-based method is applied. Multiple models are built based on different maneuvers. To predict lane-changing trajectories in highways, an IMM-based method with two maneuver states of lane-changing and lane-keeping is proposed. The method could reflect the motion characteristics of vehicles comprehensively [7]. For the uncertainty in the prediction progress, the local filter of IMM is defined, the states of the vehicles are predicted by fusing the driver behavior models [8]. The IMM-based method can effectively predict vehicle trajectories under various vehicle maneuvers in the short-term. In long-term predictions, the prediction error increases due to the changing driver's intention. In order to predict for a long time, a physics-based and maneuver-based approach is proposed. The physics-based model ensures the accuracy of short-term trajectory, and the maneuver-based model combines driving intention for long-term prediction [9], [10]. Through the trajectory prediction, the specific positions of lane-changing vehicles could be obtained in advance, while a safe path planning could be achieved.

For the lane-changing behaviors prediction, it only predicts whether lane-changing behaviors will occur in the future. Lane-changing behaviors prediction doesn't consider the specific motion state in the process of behaviors, making it more stable and suitable for complex environments. In the research area of behaviors prediction, data-based methods are widely applied. To classify and predict vehicle behaviors, an approach to predicting driver's intention based on the hidden Markov model (HMM) is presented. The approach can recognize six maneuvers including lane-changing and predict the intention

Manuscript received XX, 2020. This work was supported by the National Natural Science Foundation of China (Grant No.51975048, No.52005039, No. U1764257), and the Beijing Institute of Technology Research Fund Program for Young Scholars.

Weida Wang, Tianqi Qie, Chao Yang, Wenjie Liu, and Changle Xiang are with the School of Mechanical Engineering, Beijing Institute of Technology,

Beijing, 100081, China, and also with the Beijing Institute of Technology Chongqing Innovation Center, Chongqing 401120, China.

Kun Huang is with the School of Mechanical Engineering, Beijing Institute of Technology, Beijing, 100081, China, and also with Zhengzhou Yutong Bus Co., Ltd, Zhengzhou, 450000, China (Corresponding author: Chao Yang).

after around 4 seconds [11]. Because of its excellent performance in classification, a support vector machine (SVM) is used to classify and infer vehicle behaviors. The method performs well on the binary classification problem whether lane-changing or not [12]. To classify the lane-changing and lane-keeping behaviors, SVM based on Bayesian extension is proposed. This method can obtain a relatively more satisfactory prediction accuracy within 3 seconds compared with longer time before the actual maneuver [13]. A lot of neural network algorithms using big data for training are also used for behavior prediction [14]. In order to learn the driver's personalized lane-changing style, an optimized BP neural network is built. The result shows the network effectively identifies different drivers [15]. Due to the outstanding performance on time-series problems, the recurrent neural network is widely used to process the temporal dependence of the dataset to predict driving behavior. Besides, long short-term memory (LSTM) recurrent neural network is proposed to overcome gradient descent in the long-term [16]. To predict vehicle behavior at an unsignalized intersection, an LSTM neural network architecture is presented. The training and testing data are collected from an actual vehicle tracking system, and able to predict 1.3s advance [17]. To consider more comprehensive factors in modeling and training, the information of driver and environment is used. The model with the driver's gaze data is established, and the experiment shows that the accuracy of the model is higher than the model without the data [18]. Traffic environment information is fused into the driving behavior estimation by using continuous HMMs. The accuracy of prediction is significantly improved [19]. Data-based approaches mentioned above have been successfully applied to predict vehicle behaviors in a wide range. The application of driving environment and driver's information is proved to be effective in improving prediction accuracy [20].

In the above studies, the influence of driving environments and drivers on lane-changing are fully considered and verified. Great progress has been made, but few studies research the relationship between driving environments and drivers on lane-changing. In order to consider this relationship to predict lane-changing behaviors, an intelligent prediction based on fuzzy inference system (FIS) and LSTM, and a decision-making strategy are proposed for an autonomous vehicle under complex lane-changing scenes as shown in Fig.1.

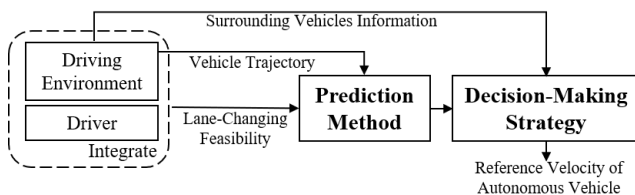


Fig. 1. The structure of proposed strategy.

In this strategy, FIS is used to simulated a driver's cognition process to the driving environments. The driving environment information is transformed into lane-changing feasibility. And then, the lane-changing feasibility and corresponding vehicle trajectory are designed as input variables of an LSTM neural network to predict the lane-changing behavior. Based on the above prediction results, an intelligent decision-making

strategy for autonomous vehicle is proposed to ensure driving safety. The contributions are given as follows.

i) A lane-changing behavior prediction method is proposed, which considers the impact and the relationship of driving environments and drivers.

ii) FIS is used to simulate drivers' cognitive processes of driving environments, which highly integrated the two factors. On the one hand, the fuzzy process and the fuzzy rules of FIS conform to people's cognitive habits, which can express the driver's cognition with driving environments. On the other hand, the fuzzy expression reduces the influence of measurement error and improves the stability of the model.

iii) An intelligent decision-making strategy combined with the intelligent prediction is proposed, which can ensure the safety of the autonomous vehicle by dynamically adjusting the vehicle motion state in advance.

iv) The performance of the proposed intelligent strategy in multiple complex driving scenarios is tested both in simulation and hardware in the loop (HIL) system environment.

This paper is organized as follows. Section II proposes the lane-changing behavior prediction method. Section III introduces the vehicle model and decision-making strategy. Section IV verifies the proposed strategy both in simulation and HIL system. Section V gives a conclusion.

II. LANE CHANGING BEHAVIORS PREDICTION

In order to predict lane-changing behaviors under complex driving environments, driving environments and drivers' information, as well as vehicle motion states are considered. And a FIS-LSTM-based prediction method is proposed.

A. Scene description for lane-changing behaviors prediction

To describe lane-changing behaviors in the complex environment, the typically lane-changing scene is described in Fig.2. In the scene, target vehicle (TV) is the predicted vehicle. The surrounding vehicles (SVs) of TV are divided into six categories according to their position relative to the TV.

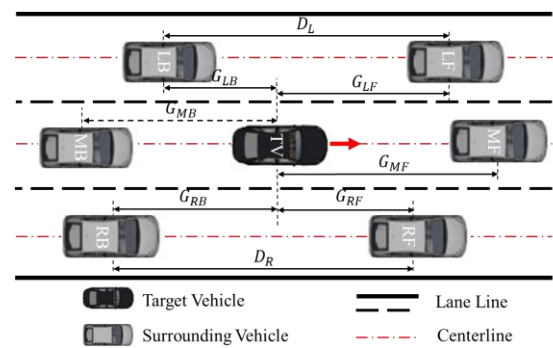


Fig. 2. The lane-changing scene

Several studies show that lane-changing involves the interaction of several vehicles [21]. And, drivers usually evaluate the lane-changing feasibility via the relative distance with SVs as shown in Fig. 2 [22]. For left lane-changing, the specific parameters of the distance are G_{MF} , G_{LF} , G_{LB} , and D_L , respectively. For right lane-changing, the parameters are G_{MF} , G_{RF} , G_{RB} , and D_R , respectively. The detailed meanings of the parameters in Fig.2 are shown in Table I.

TABLE I
MEANINGS OF PARAMETERS IN THE LANE-CHANGING SCENE

Parameters	Meaning
$G_{LF}/G_{MF}/G_{RF}$	The gaps between TV and the vehicle ahead in left/middle/right lane.
$G_{LB}/G_{MB}/G_{RB}$	The gaps between TV and the vehicle behind in left/middle/right lane.
D_L/D_R	The distances between the vehicle ahead and behind in left/right lane.
TV	The target vehicle which is predicted.
LF/MF/RF	The vehicle in front of TV in left/ middle/ right lane.
LB/MB/RB	The vehicle behind TV in left/ middle/ right lane.

B. Lane-changing feasibility evaluation

For lane-changing behaviors, driving environment and the driver of predicted vehicle are the two main factors. Driving environment represents the objective factor. And, the driver represents the subjective factor, indicating how the driver cognize the objective environment. In this section, lane-changing feasibility is defined to express driver's cognition of the driving environment.

To model the driver's cognition progress, FIS is applied, which establishes a relationship between the parameters of the environment and the lane-changing feasibility. Firstly, generally the relative distance of some surrounding vehicles is the main factor for drivers to judge whether to change lanes. Therefore, the gap distances are selected as inputs of FIS. Secondly, the input membership functions of FIS transform the specific values of gaps and distances to fuzzy values, which accords with the driver's understanding of the environment. Thirdly, the fuzzy rules of the FIS are designed based on the driver's judgment of the environment [22].

Taking left lane-changing as an example, G_{MF} , G_{LF} , G_{LB} , and D_L are regarded as the inputs of the FIS, and the feasibility of left lane-changing is set as the output, which are connected by input membership functions, fuzzy rules, and output membership functions [21].

The fuzzy membership functions are shown in Fig. 3. The input membership functions transform the specific values of gaps and distances to fuzzy values, which are represented as close, medium, and far. They are shown as Fig. 3(a).

The output membership functions represent the relationship between the feasibility of lane-changing and the values processed by fuzzy rules. They are shown as Fig. 3(b) [22].

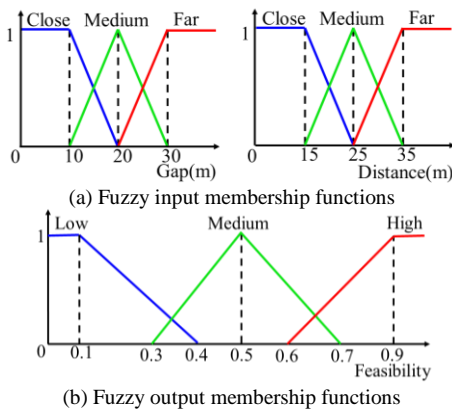


Fig. 3. Fuzzy membership functions

The fuzzy rules of the FIS are designed based on the driver's cognition, which is verified can represent the driver's

evaluation of the lane-changing feasibility by a research [22]. As shown in Table II, for left lane changing, the i th rule indicates as follows.

R_i : IF (G_{LF} is b_i) and (G_{LB} is c_i) and (D_L is e_i) and (G_{MF} is f_i)
THEN (LCF is g_i) (1)

where b_i , c_i , e_i , and f_i represent the inputs of fuzzy rules, respectively. The input variables include close, medium, and far. g_i represents the output of fuzzy rules, which include low, medium, and high. LCF represents left lane-changing feasibility.

TABLE II
FUZZY RULES

R_i	IF				THEN
	G_{LB}	G_{LF}	D_L	G_{MF}	LCF
1	Close	Close	Close	Close	Low
2	Close	Medium	Close	Close	Medium
3	Close	Close	Medium	Close	Medium
4	Close	Close	Far	Close	High
5	Close	Close	Close	Medium	Low
6	Close	Close	Close	Far	Low
7	Close	Medium	Medium	Medium	Medium
8	Close	Far	Far	Far	Medium
9	Close	Close	Medium	Medium	Medium
10	Close	Close	Medium	Far	Low
11	Close	Close	Far	Medium	Medium
12	Close	Medium	Close	Medium	Low
13	Close	Medium	Far	Close	High
14	Close	Medium	Far	Medium	High
15	Close	Medium	Far	Far	Medium
16	Close	Medium	Medium	Close	Medium
17	Close	Far	Far	Close	High
18	Close	Medium	Medium	Far	Low
19	Close	Medium	Close	Far	Low
20	Close	Medium	Medium	Far	Low
21	Close	Far	Far	Medium	High
22	Close	Far	Medium	Far	Low
23	Medium	Medium	Medium	Medium	Medium
24	Medium	Close	Medium	Medium	Medium
25	Medium	Medium	Far	Medium	High
26	Medium	Medium	Medium	Far	Low
27	Medium	Medium	Medium	Close	High
28	Medium	Far	Far	Far	Medium
29	Medium	Medium	Far	Far	Medium
30	Medium	Close	Medium	Close	Medium
31	Medium	Far	Far	Medium	High
32	Medium	Medium	Far	Close	High
33	Medium	Close	Far	Close	Low
34	Medium	Close	Far	Medium	Medium
35	Medium	Close	Medium	Far	Low
36	Medium	Close	Close	Far	Low
37	Medium	Far	Far	Close	High
38	Medium	Close	Close	Close	Low
39	Far	Far	Far	Far	Medium
40	Far	Medium	Medium	Medium	Medium
41	Far	Close	Far	Far	Medium
42	Far	Medium	Far	Far	Medium
43	Far	Far	Medium	Far	Medium
44	Far	Far	Far	Close	High
45	Far	Far	Far	Medium	High
46	Far	Far	Medium	Medium	Medium
47	Far	Close	Far	Close	High
48	Far	Medium	Far	Medium	High
49	Far	Medium	Far	Close	High
50	Far	Close	Medium	Close	High
51	Far	Close	Medium	Medium	Middle

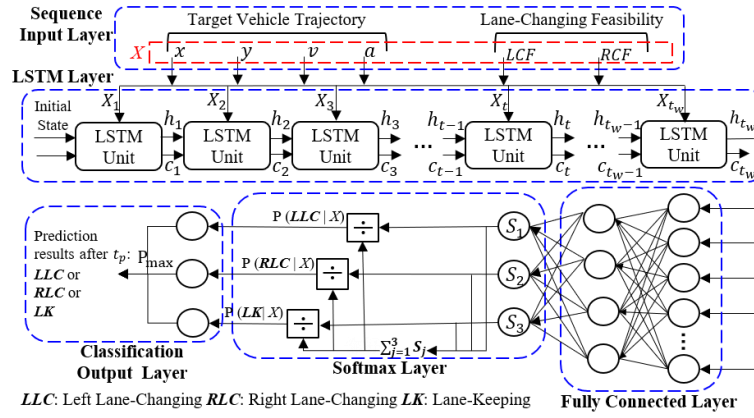


Fig. 4. Structure of lane-changing behavior prediction model

C. Lane-changing behaviors prediction

In order to predict lane-changing behavior, a model based on FIS-LSTM is established. The structure of the model contains five layers, which are shown in Fig. 4. The first layer is the sequence input layer, in which the input time series variables are imported. And, the length of time series is represented by time window, t_w . The data for each time step is as follows.

$$X = [x, y, v, a, LCF, RCF] \quad (2)$$

where x and y donate lateral and longitudinal coordinate of the predicted vehicle, respectively. v is the vehicle velocity, a represents the vehicle acceleration, RCF represents right lane-changing feasibility

The second layer is LSTM layer, which is composed of the LSTM cell. The third layer is a fully connected layer, and the activation function is ReLU. The fourth layer is a softmax layer. After being processed by the softmax layer, the probability matrix of lane-changing behavior is concluded.

$$\Omega = [\omega_1, \omega_2, \omega_3] \quad (3)$$

where ω_1 , ω_2 and ω_3 represent the probability of *left lane-changing*, *right lane-changing*, and *lane-keeping*, respectively.

The fifth layer is the classification output layer, which exports the results of lane-changing behaviors prediction after prediction time, t_p .

LSTM layer is core of the proposed method. The LSTM cell structure is employed as shown in Fig. 5 [23]. The input is the cell state of the former time step C_{t-1} , the output of the former time step h_{t-1} , and the current input x_t , respectively. In order to process time-series data, simple linear transformation and gate structure of the cell state are added. The calculation procedures of the LSTM cell include three gates. forget gate, input gate, and output gate, respectively. In these procedures, σ and \tanh can be represented as follows.

$$\sigma(x) = \frac{1}{1+e^{-x}} \quad (4)$$

$$\tanh(x) = \frac{e^x - e^{-x}}{e^x + e^{-x}} \quad (5)$$

The forget gate determines what information is forgotten. f_t represents the forget gate, which is defined as follows.

$$f_t = \sigma(W_f \times [h_{t-1}, x_t] + b_f) \quad (6)$$

where W_f is the weight matrix of the forget gate, and b_f is the bias of the forget gate.

The input gate determines whether the current input will contribute to the cell state or not, which can be denoted as.

$$i_t = \sigma(W_i \times [h_{t-1}, x_t] + b_i) \quad (7)$$

$$\tilde{C}_t = \tanh(W_C \times [h_{t-1}, x_t] + b_C) \quad (8)$$

where i_t represents the input gate, W_i is the weight matrix of the input gate, b_i is the bias of the input gate, and \tilde{C}_t is an estimation of the new cell state value.

The output gate controls the candidate output, which can be defined as follows.

$$o_t = \sigma(W_o \times [h_{t-1}, x_t] + b_o) \quad (9)$$

$$C_t = f_t \times C_{t-1} + i_t \times \tilde{C}_t \quad (10)$$

$$h_t = o_t \times \tanh(C_t) \quad (11)$$

where W_i is the weight matrix of the output gate, and b_i is the bias of the output gate.

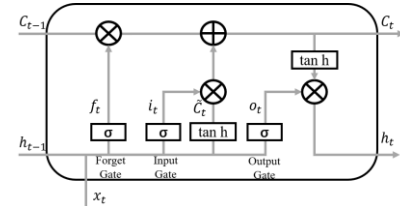


Fig. 5. The LSTM cell structure

III. DECISION-MAKING STRATEGY FOR AN AUTONOMOUS VEHICLE BASED ON PREDICTION

To ensure the driving safety of autonomous vehicle, an obstacle-free area ahead is necessary. If some other vehicle changes lane into this obstacle-free area, the autonomous vehicle may not have enough time to make decisions and carry out it to deal with this action. Sudden braking or even collision might occur, which would directly affect the driving safety and comfort. If the lane-changing action is accurately predicted and the corresponding decision is made in advance, the autonomous vehicle will have enough time to avoid risks [24], [25]. Thus, a decision-making strategy is proposed to deal with different prediction results in the following subsections.

A. Finite State Machine of Driving states

In the part, a finite state machine is proposed to represent different vehicle states. The states transition is based on the prediction results of TVs and the real-time perception information of the autonomous vehicle shown in Fig. 6. The following distance and safe distance of the autonomous vehicle is represented in Fig. 6, which are defined later. Different numbers on vehicles is used to distinguish them.

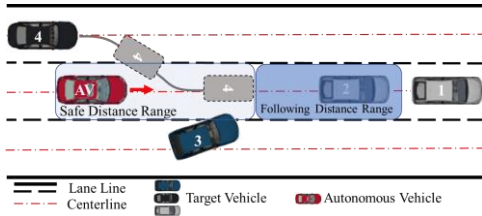


Fig. 6. Vehicle positions in different driving scenes

According to the different driving scenes, four vehicle states are defined as follows, and shown in Fig. 7.

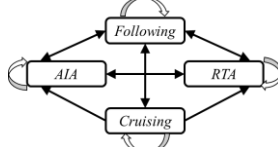


Fig. 7. Finite state machine of vehicle states

i) *Cruising*: If the distance between the autonomous vehicle and the preceding vehicle (1) as shown in Fig.7 is longer than the cruising distance, the autonomous vehicle will in a *Cruising* state. The cruising distance is described as follows.

$$D_C = D_{C0} + \gamma v_{AV} \quad (12)$$

where D_C is cruising distance, D_{C0} is basic cruising distance, v_{AV} is the velocity of the autonomous vehicle, and γ is the velocity factor of cruising distance.

ii) *Following*: If the preceding vehicle (2) is within the following distance range, the autonomous vehicle will in the *Following* state, which is represented as follows.

$$D_s < y_{pre} - y_{AV} \leq D_C \quad (13)$$

where y_{pre} and y_{AV} are the longitudinal positions of preceding vehicle and autonomous vehicle, respectively, D_s is safe distance, which will be described in detail in the following.

iii) *Real-time avoidance (RTA)*: If a vehicle (3) is detected to be within the safe distance range of the autonomous vehicle, the vehicle state will become *RTA* state. The safe distance is the range of obstacle free area.

$$D_s = D_{s0} + \beta v_{AV} \quad (14)$$

where D_s is safe distance, D_{s0} is basic following distance, and β is the velocity factor of safe distance.

iv) *Avoidance in advance (AIA)*: If the prediction result shows that a vehicle (4) will drive into the safety distance range, the vehicle state will become *AIA* state.

Since the lane-changing time is short and the velocity change is small, the vehicle velocity is assumed constant during lane-changing. The positions of TV and the autonomous vehicle at the end of lane-changing process are defined as follows:

$$y_{TV}^{t_0+t_p} = y_{TV}^{t_0} + v_{TV}^{t_0} t_p \quad (15)$$

$$y_{AV}^{t_0+t_p} = y_{AV}^{t_0} + v_{AV}^{t_0} t_p \quad (16)$$

where y_{TV}^t and y_{AV}^t represent the longitudinal positions of TV and autonomous vehicle at time t , respectively. v_{TV}^t and v_{AV}^t donate the velocity of TV and autonomous vehicle at time t , respectively, t_0 is the start time of lane-changing predict.

If the relative position between TV and the autonomous vehicle meets the constraint described in the following equation, *AIA* will be carried out.

$$0 < y_{TV}^{t_0+t_p} - y_{AV}^{t_0+t_p} \leq D_s \quad (17)$$

The state of the autonomous vehicle is mainly based on two factors. One is the lane-changing prediction results of TVs, and the other is the distance between autonomous vehicle and vehicle ahead. The detailed strategy transition among the four state is shown in *Algorithm 1*.

Algorithm 1

```

1: Input prediction results  $P_R$ , current driving state  $M_{cd}$ , the distance
   between autonomous vehicle and vehicle ahead  $D$ .
2: if  $M_{cd}$  is Cruising then
3:   if  $D \leq D_s$  then
4:      $M_{cd}$  becomes RTA
5:   else if  $P_R$  is lane-changing and
6:      $0 < y_{TV}^{t_0+t_p} - y_{AV}^{t_0+t_p} \leq D_s$  then
7:      $M_{cd}$  becomes AIA
8:   else if  $D \leq D_C$  then
9:      $M_{cd}$  becomes Following
10:  else  $M_{cd}$  keeps Cruising
11:  end if
12: else if  $M_{cd}$  is Following then
13:   if  $D \leq D_s$  then
14:      $M_{cd}$  becomes RTA
15:   else if  $P_R$  is lane-changing and
16:      $0 < y_{TV}^{t_0+t_p} - y_{AV}^{t_0+t_p} \leq D_s$  then
17:      $M_{cd}$  becomes AIA
18:   else if  $D > D_C$  then
19:      $M_{cd}$  becomes Cruising
20:   else  $M_{cd}$  keeps Following
21:   end if
22: else if  $M_{cd}$  is RTA then
23:   if  $D \leq D_s$  then
24:      $M_{cd}$  keeps RTA
25:   else if  $P_R$  is lane-changing and
26:      $0 < y_{TV}^{t_0+t_p} - y_{AV}^{t_0+t_p} \leq D_s$  then
27:      $M_{cd}$  becomes AIA
28:   else  $M_{cd}$  becomes Following
29:   end if
30: else if  $M_{cd}$  is AIA then
31:   if  $D \leq D_s$  then
32:      $M_{cd}$  becomes RTA
33:   else if  $P_R$  is lane-changing then
34:      $M_{cd}$  keeps AIA
35:   else  $M_{cd}$  becomes Following
36:   end if
37: end if

```

B. Reference velocity planning

In this part, the reference velocity of the autonomous vehicle under each state are planned. The design principle of proposed planning strategy is to keep the autonomous vehicle a safe distance from the vehicle ahead. The detailed descriptions will be given as follows.

In *Cruising* state, the velocity of the autonomous vehicle is the set cruising velocity.

$$v_{AV,ref}^t = v_C \quad (18)$$

where v_C is cruising velocity.

In *Following* state, the autonomous vehicle will follow the vehicle ahead. The reference following distance is the expected distance from the autonomous vehicle to front vehicle.

$$D_F = D_{F0} + \alpha v_{AV} \quad (19)$$

where D_F is reference following distance, D_{F0} is basic following distance, and α is the velocity factor of following distance.

The reference velocity is planned as follows.

$$v_{AV,ref}^t = v_{HV}^t + \delta(D_t - D_F) \quad (20)$$

where $v_{AV,ref}^t$ is the reference velocity of the autonomous vehicle at time t , v_{HV}^t is the velocity of vehicle ahead at time t , D_t is the distance between autonomous vehicle and the vehicle ahead at time t , δ is velocity adjustment factor.

In *RTA* state, obstacles are not predicted, and suddenly appear within the safe distance. In response to this situation, the vehicle will brake emergency with the maximum deceleration.

The reference velocity is described as follows.

$$v_{AV,ref}^t = v_{0,RTA} - \int_{t_{0,RTA}}^t a_{dmax}(t) dt \quad (21)$$

where $v_{0,RTA}$ and $t_{0,RTA}$ are the initial velocity of the autonomous vehicle and the time when the vehicle becomes *RTA* state. a_{dmax} is maximum deceleration that can be achieved without wheel locking.

In *AIA* state, the vehicle that will change lane is known, the distance between the two vehicles can be adjusted in advance. To obtain enough obstacle-free area, the velocity of autonomous vehicle should meet the following equation.

$$\int_{t_{0,AIA}}^{t_{0,AIA}+t_p} [v_{TV}(t) - v_{AV}(t)] dt = D_F - D_{0,AIA} \quad (22)$$

where $t_{0,AIA}$ donates the time when the vehicle becomes *AIA* state, $D_{0,AIA}$ is the initial distance between TV and autonomous vehicle when the vehicle becomes *AIA* state.

During the process of obstacle avoidance, the autonomous vehicle is planned to motion with uniform deacceleration. The reference velocity at time t is computed as follows.

$$v_{AV,ref}^t = v_{TV}^t - \frac{2(D_F - D_t)}{t_p - (t - t_{0,ATA})} \quad (23)$$

where, v_{TV}^t is the velocity of the target vehicle at time t .

IV. RESULTS AND DISCUSSION

In this section, firstly, the prediction method based on FIS and LSTM is trained and tested to evaluate the performance of the method. Secondly, to verify the decision-making strategy based on the prediction results, the HIL system is built. Thirdly, the prediction and decision-making strategy are applied in real driving scenes in HIL system.

A. Simulation results

In order to train and test the prediction method, the NGSIM dataset is used [18]. The NGSIM dataset contains a large number of detailed vehicle trajectory data including lateral and longitudinal coordinate, velocity, acceleration, current lane position of vehicles, and so on. To obtain the data with different lane-changing behaviors of vehicles, the dataset is classified and standardized. Among them, 75% of the data is used for training and 25% is used for testing. The NGSIM dataset contains various scenarios, such as different traffic flow and vehicle speed, which could ensure the method is generally effective in different scenarios.

The schematic diagram of prediction process is shown in Fig. 8. The prediction data consists of two parts. One is the prediction time sequence, the other is the reference prediction result, which is right lane-changing in Fig. 8. The prediction time sequence is regarded as input of the proposed prediction method, and the output is compared with the reference prediction result. If they are the same, the prediction is correct. On the contrary, the prediction is incorrect.

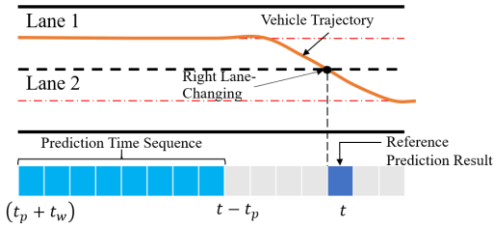


Fig. 8. Diagram of prediction process

In the case of using different prediction time t_p and time window t_w , the prediction accuracy is shown in Fig. 9. The prediction accuracy could be defined as follows.

$$\text{Accuracy} = \frac{N_{right}}{N_{test}} \quad (24)$$

where N_{test} is a total number of test data samples, N_{right} is the number of test data samples that can correctly predict lane-changing behaviors.

As shown in Fig. 9, the test accuracy can be improved by selecting the appropriate t_w . For example, when $t_p = 2s$, the highest accuracy is achieved in the case of $t_w = 2.5s$. For different t_p , the best accuracy could be achieved with the best fitted t_w is shown in Table III. Although with the increase of t_p , the accuracies of the prediction decrease, they are higher than 92% in all cases.

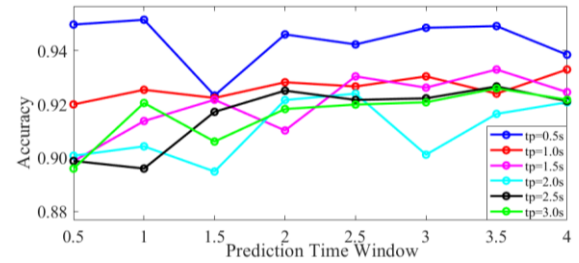


Fig. 9. The prediction accuracy

TABLE III
BEST ACCURACY ACHIEVED

t_p (s)	Best Fitted t_w (s)	Best Accuracy achieved
0.5	1.0	0.9515
1.0	4.0	0.9330
1.5	3.5	0.9330
2.0	2.5	0.9240
2.5	3.5	0.9266
3.0	3.5	0.9259

Compared with proposed method, two methods without FIS is simulated. One of them uses only vehicle trajectory data. The data for each time step is as follows.

$$X_1 = [x, y, v, a] \quad (25)$$

The other uses all data without the processes of FIS. The data for each time step is as follows.

$$X_2 = [x, y, v, a, G_{LF}, G_{LB}, G_{MF}, G_{RF}, G_{RB}, D_L, D_R] \quad (26)$$

The best accuracy could be achieved of the methods is shown in Table IV. The best accuracy could be achieved by proposed method is significantly higher than the other methods.

TABLE IV
BEST ACCURACY ACHIEVED OF THE METHODS

t_p (s)	Best Accuracy achieved (X)	Best Accuracy achieved (X_1)	Best Accuracy achieved (X_2)
0.5	0.9515	0.6353	0.7887
1.0	0.9330	0.6380	0.7693
1.5	0.9330	0.6420	0.7760
2.0	0.9240	0.6413	0.7620
2.5	0.9266	0.6627	0.7620
3.0	0.9259	0.6520	0.7820

B. HIL system setup

The performance of a lane-changing behavior prediction method and decision-making strategy in the real driving scenes are verified via a HIL system. The layout of the HIL system is shown in Fig. 10. The system is consisted of workstation, controller area network (CAN) data collector, controller, low-voltage power supply, camera, and scene display screen. In the system, driving scenes are established in a workstation, and displayed on the screen. The camera perceives the scene information on the screen. The controller is used to operate the prediction method and the decision-making strategy. The low-voltage power supply is responsible for powering the controller and camera via direct current (DC) power line. CAN-bus is used for information transmission among workstation, controller, and camera. The configuration of the above components is shown in Table V.

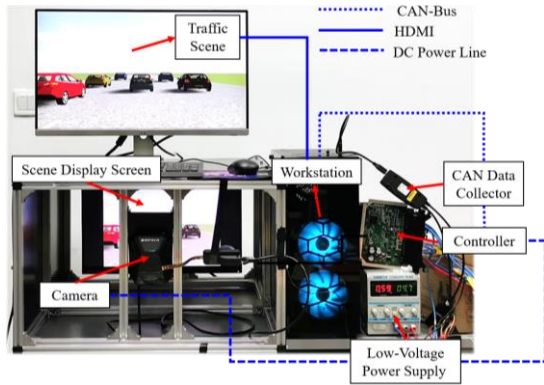


Fig. 10. The layout of HIL system

TABLE V
THE CONFIGURATION OF HIL SYSTEM

Component	Configuration
Workstation	CPU, Intel(R) Core (TM) i7-10700 CPU @2.90GHz, RAM, 16GB
CAN data collector	Kvaser memorator professional HS/LS
Low-voltage power supply	Voltage, 10VDC, Current, 0.60A
Camera	Mobileye mb6
Controller	NXP Semiconductors MPC5744P-144DS

According to the function, the HIL system is divided into four modules as shown in Fig. 11. They are scene establishment module, scene display module, scene perception module, decision-making, and control module, respectively. In the driving scene establishment module, the driving scene is built in workstation with PreScan using the data collected in the real driving scene. And then, the scene is transformed into a first-person perspective, and displayed on a screen. In the scene perception module, the driving environment information can be obtained in two ways. One is the perception of the camera, and the other is to build the communication network between vehicles. According to the driving environment, in decision-making and control module, the lane-changing behavior prediction method and decision-making strategy will be operated in a designed controller. The control method referred to in the existing literature also runs in the controller [26].

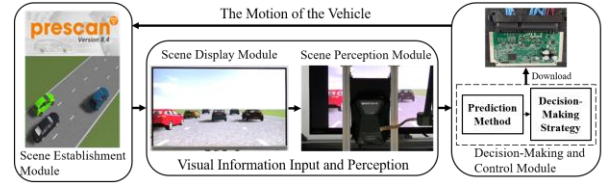


Fig. 11. Function diagram of HIL system

C. HIL Test

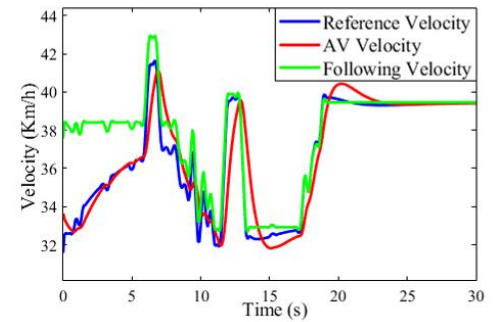
To simulation the real driving environment, the scene is constructed in the HIL according to the typical lane-keeping (following) and lane-changing (cut-in) scenario in the NGSIM dataset. The proposed strategy is applied in the scenarios and compared with the human driver. In the test, the relevant parameters of prediction and decision-making strategy are shown in TABLE VI.

TABLE VI
THE PARAMETERS VALUE OF THE TEST

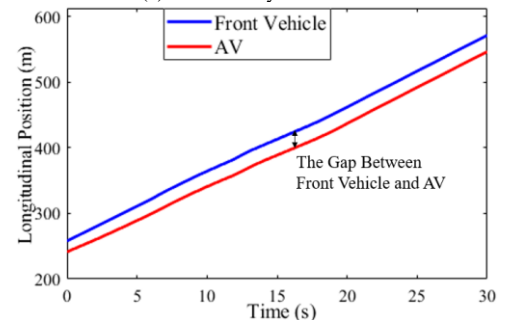
Parameters	Value
t_p	3s
D_F	25m
D_s	15m

Case 1: When the front vehicle is in the following distance range of AV as shown in Fig. 6, the *Following* state of proposed strategy is applied.

HIL test results are shown in Fig. 12. As shown in Fig. 12(a), the following velocity represents the velocity of the front vehicle. The reference velocity is the velocity of the front vehicle, which changes frequently between 32Km/h and 43Km/h. Based on the following velocity and the gap between vehicles, the reference velocity is computed to keep a safe distance from the front vehicle. The AV velocity is controlled based on the reference velocity, which has good tracking performance. The longitudinal position of the front vehicle and AV is shown in Fig. 12(b). And the gap between the two vehicles is shown in Fig. 12(c). The initial gap is 16.7m. Applied the *Following* state, it keeps increasing until the gap reaches D_F .



(a) The velocity of vehicles



(b) The longitudinal position of vehicles

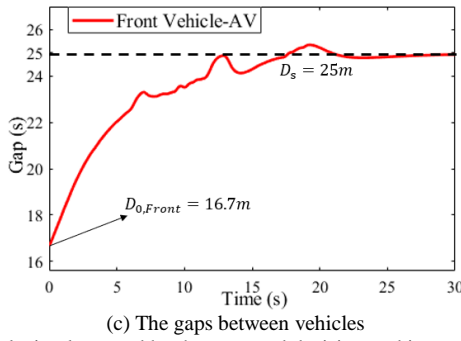


Fig. 12. Results implemented by the proposed decision-making strategy in the following scenarios

Case 2: The scenarios is shown in Fig. 13(a). Four vehicles associated with lane-changing are included, TV, MF, RF, and RB mentioned in Fig. 2. Among them, TV is a lane-changing vehicle. RB is an autonomous vehicle to execute the decision-making strategy, which is also represented as AV.

The HIL test results implemented by human driver are shown in Fig. 13. To show the prediction results clearly, the definition is made that, the time when TV crosses the lane line is 0. As shown in Fig. 13(a), the same marks represent the same time. And the obvious lateral position movement of TV appears at -0.25 s. Before 0s, human driver doesn't respond to lane-changing and still accelerate until TV completes the lane-changing. After 0s, TV runs between AV and RF as shown in Fig. 13(c), which makes TV need to keep a gap from RF. The gap results are shown in Fig. 13(d). Obviously, driver adjusts TV velocity frequently to maintain a safe gap. The significant decelerations of TV appear both at 3-5s and 11-13s shown in Fig. 13(b). When TV decelerates, the gap between TV and AV will reduce as shown in Fig. 13(b). Then, at 5-7s and 13-14s, AV decelerate and the gap between TV and AV increase, which indicates that the deceleration of TV and AV has an obvious corresponding relationship. As shown in Fig. 13(d), the deceleration of AV has a time-delay compared with that of TV, resulting in the two vehicles being close at some moment, such as at 6s and 13s. The gap result between vehicles is within 10-20m as shown in Fig. 13(d).

The results of applying the proposed strategy is shown in Fig. 14. The state of AV is decided according to the prediction result

and driving environment, which include AIA state and Following state. At -3 s, TV is predicted to change lane at 0s. Judging by the decision-making strategy, AV becomes AIA state. After lane-changing, AV becomes Following state at 0s, according to the distance between AV and TV. Based on the vehicle state, the reference velocity is computed as shown in Fig. 14(a). The motion of AV is controlled based on the reference velocity, and the AV velocity is shown in Fig. 14(a). In AIA state, the initial distance at the start of the state is 18.8m as shown in Fig. 14(c). The gap between TV and AV keeps increasing in the state. At the end of AIA state, the gap is 26.2m. Compared with results implemented by human driver, the AV in AIA state decelerates at the prediction time, which could keep a safe distance with TV before the lane-changing. Moreover, although the reference velocity of AV is less than 0 in some cases, the actual velocity is still more than 0 due to the constraints of actuating control. In Following state, the gap between TV and AV is within 24-26m, which is stable at around 25m. Compared with results implemented by human driver, the gap fluctuation is smaller, which could respond to the changeable TV velocity in time. And, the velocity variation in Following state is gentler than that in human driving process as shown in Fig. 14(a).

The results of applying the proposed strategy without lane-changing behaviors prediction are shown in Fig. 15. The state of AV is decided only according to the driving environment, which applies *Following* state. TV in this situation represents the vehicle in front of AV. The reference velocity and actual velocity of AV is shown in Fig. 15(a). The longitudinal position of vehicles is shown in Fig. 15(b). At 0s, a vehicle changes lane, and the longitudinal of TV suddenly decreases due to the change of front vehicle. The gap between TV and AV is shown in Fig. 15(c). The gap decreases to 15.3m at 0s which is smaller than 26.2m obtained in the previous strategy. After lane-changing, the gap increases to about 25m. Compared with the proposed strategy with prediction, the strategy could not avoid lane-changing vehicles in advance, which lead to the sudden gap change between TV and AV.

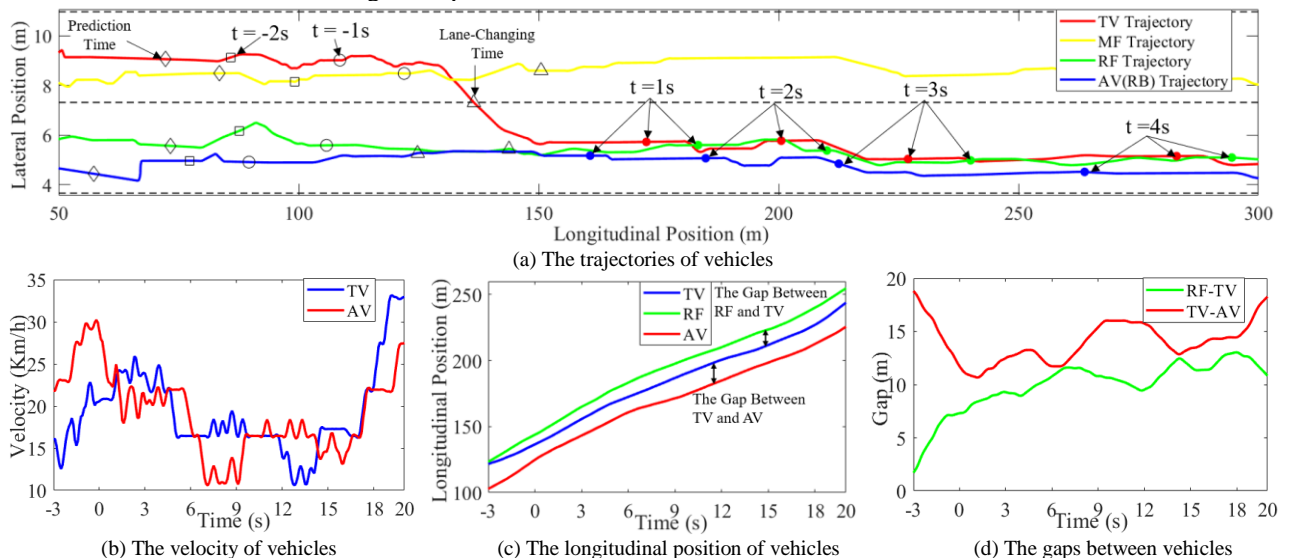


Fig. 13. Results implemented by human driver in the cut-in scenario

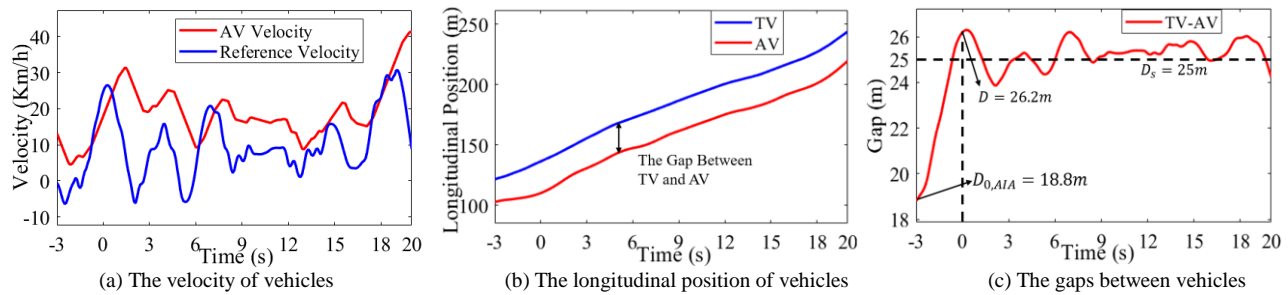


Fig. 14. Results implemented by the proposed decision-making strategy in the cut-in scenario

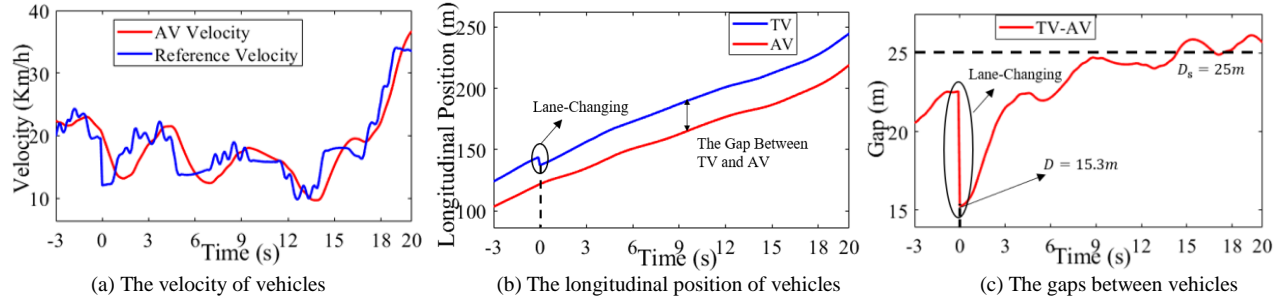


Fig. 15. Results implemented by the proposed decision-making strategy without prediction in the cut-in scenario

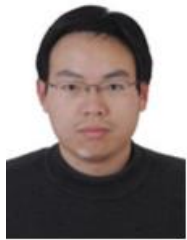
V. CONCLUSION

The paper presents a FIS-LSTM method to predict lane-changing behaviors. The interaction between vehicles and drivers are considered by proposed FIS-LSTM method. The prediction method is trained and tested by the NGSIM dataset. The accuracy of the prediction in different conditions can reach 92.40%. On the basis of the prediction results, a decision-making strategy with full consideration of driving safety and comfort is given. The strategy is verified in the HIL system compared with the human driver, and results show that the vehicle using the proposed strategy keeps a safe distance from the surrounding vehicles. In addition, owing to the prediction, lane-changing behaviors of surrounding vehicles can be known in advance, the autonomous vehicle has enough reaction time. The change of planned vehicle velocity and acceleration in autonomous vehicle is gentler than that of human driving vehicles, which indicates the proposed strategy is effective to improve the driving safety and comfort. The proposed strategy has the potentials for application in actual vehicle controller.

REFERENCES

- [1] C. Yang, M. Zha, W. Wang, K. Liu and C. Xiang, "Efficient energy management strategy for hybrid electric vehicles/plug-in hybrid electric vehicles: review and recent advances under intelligent transportation system," *IET Intell. Transp. Sy.*, vol. 14, no. 7, pp. 702–711, Feb 2020.
- [2] A. Benloucif, A.-T. Nguyen, and C. Sentouh, "Cooperative trajectory planning for haptic shared control between driver and automation in highway driving," *IEEE Trans. Ind. Electron.*, vol. 66, no. 12, pp. 9846-9857, Dec. 2019.
- [3] X. Wang, J. Liu, and T. Qiu, "A real-time collision prediction mechanism with deep learning for intelligent transportation system," *IEEE Trans. Veh. Technol.*, vol. 69, no. 9, pp. 9497-9508, Sep. 2020.
- [4] Y. Xing, C. Lv, and H. Wang, "Driver lane change intention inference for intelligent vehicles: framework, survey, and challenges," *IEEE Trans. Veh. Technol.*, vol. 68, no. 5, pp. 4377-4390, May. 2019.
- [5] M. Brännström, E. Coelingh, and J. Sjöberg, "Model-based threat assessment for avoiding arbitrary vehicle collisions," *IEEE Trans. Intell. Transp. Syst.*, vol. 11, no. 3, pp. 658-669, Sep. 2010.
- [6] J. Kim, and D. Kum, "Collision risk assessment algorithm via lane-based probabilistic motion prediction of surrounding vehicles," *IEEE Trans. Intell. Transp. Syst.*, vol. 19, no. 9, pp. 1-10, Sep. 2018.
- [7] R. T-Moreo, and M. A. Z-Izquierdo, "IMM-based lane-change prediction in highways with low-cost GPS/INS," *IEEE Trans. Intell. Transp. Syst.*, vol. 10, no. 1, pp. 1-10, Mar. 2009.
- [8] Y. Jeong, and K. Yi, "Target vehicle motion prediction-based motion planning framework for autonomous driving in uncontrolled intersections," *IEEE Trans. Intell. Transp. Syst.*, pp. 1-10, Dec. 2019.
- [9] R. Huang, H. Liang, and P. Zhao, "Intent-estimation- and motion-model-based collision avoidance method for autonomous vehicles in urban environments," *Appl. Sci.*, vol.7, no.9, pp. 457-477, Apr. 2017.
- [10] G. Xie, H. Gao, and L. Qian, "Vehicle trajectory prediction by integrating physics- and maneuver-based approaches using interactive multiple models," *IEEE Trans. Ind. Electron.*, vol. 65, no.7, pp. 5999–6008, Jul 2018.
- [11] D. Tran, L. Liu, and M. Liu, "A hidden markov model based driver intention prediction system," in *Proc IEEE Int. Conf. on CYBER Technology in Automation, Control, and Intelligent Systems*, 2015.
- [12] P. Kumar, M. Perrollaz, and S. Lefèvre, "Learning-based approach for online lane change intention prediction", in *Proc. IEEE Intell. Vehicles Symp.*, 2013, pp. 797-802.
- [13] B. Morris, A. Doshi, and M. Trivedi, "Lane change intent prediction for driver assistance: On-road design and evaluation," in *Proc. IEEE Intell. Vehicles Symp.*, 2011, pp. 895–901.
- [14] F. Lethaus, M. R. K. Baumann, and F. Köster, "Using pattern recognition to predict driver intent," in *Proc. Int. Conf. Adaptive Natural Comput. Algorithms*, 2011, pp. 140–149.
- [15] B. Zhu, S. Yan, and J. Zhao, "Personalized lane-change assistance system with driver behavior identification," *IEEE Trans. Veh. Technol.*, vol. 67, no. 11, pp. 10293-10306, Nov. 2018.
- [16] Y. Xing, C. Lv, and D. Cao, "Personalized vehicle trajectory prediction based on joint time-series modeling for connected vehicles," *IEEE Trans. Veh. Technol.*, vol. 1, no. 2, pp. 1341-1352, Feb. 2020.
- [17] A. Zyner, S. Worrall, and E. Nebot, "A recurrent neural network solution for predicting driver intention at unsignalized intersections," *IEEE Robot. Autom. Lett.*, vol. 3, no. 3, pp. 1759-1764, Jul. 2018.
- [18] X. Li, W. Wang, and M. Roetting, "Estimating driver's lane-change intent considering driving style and contextual traffic," *IEEE Trans. Intell. Transp. Syst.*, vol. 20, no. 9, pp. 3258-3271, Sep. 2019.
- [19] Y. Zhang, Q. Lin, and J. Wang, "Lane-change intention estimation for car-following control in autonomous driving," *IEEE Trans. Intell. Vehicles*, vol. 3, no. 3, pp. 276–286, Sep. 2018.

- [20] C. Yang, S. You, and W. Wang, "A Stochastic Predictive Energy Management Strategy for Plug-in Hybrid Electric Vehicles based on Fast Rolling Optimization," *IEEE Trans. Ind. Electron.*, vol. 67, no. 11, pp. 9659-9670, Nov. 2020.
- [21] Y. Bian, S. Li, and W. Ren, "Cooperation of multiple connected vehicles at unsignalized intersections: distributed observation, optimization, and control," *IEEE Trans. Ind. Electron.*, vol. 67, no. 12, pp. 10744-10754, Apr. 2019.
- [22] E. Balal, R. L. Cheu, and T. S-Gyan, "A binary decision model for discretionary lane changing move based on fuzzy inference system," *Transl. Res.*, vol. 68, pp. 47-61, June. 2016.
- [23] A. Zyner, S. Worrall, and E. Nebot, "A recurrent neural network solution for predicting driver intention at unsignalized intersections," *IEEE Robot. Autom. Lett.*, vol. 3, no. 3, pp. 1759-1764, Jul. 2018.
- [24] S. Noh, "Decision-making framework for autonomous driving at road intersections: safeguarding against collision, overly conservative behavior, and violation vehicles," *IEEE Trans. Ind. Electron.*, vol. 66, no. 4, pp. 3275-3286, Apr. 2019.
- [25] Y. Huang, H. Ding, and Y. Zhang, "A motion planning and tracking framework for autonomous vehicles based on artificial potential field elaborated resistance network approach," *IEEE Trans. Ind. Electron.*, vol. 67, no. 2, pp. 1376-1386, Feb. 2020.
- [26] R. Marino, S. Scalzi, and M. Netto, "Nested PID steering control for lane keeping in autonomous vehicles," *Control Eng. Practice*, vol. 16, no. 12, pp. 1459-1467, Dec. 2011.



Weida Wang received the Ph.D. degree from Beihang University, Beijing, China, in 2009. He is currently an associate professor with the School of Mechanical Engineering, Beijing Institute of Technology, Beijing, China. He is the Director of Research Institute of Special Vehicle, Beijing Institute of Technology, Beijing, China. His current research interests include hybrid vehicle, electromechanical transmission control, and energy management strategy.



Tianqi Qie received the B.S. degree from Beijing Institute of Technology, Beijing, China, in 2019. She is currently working toward the M.S. degree with the School of Mechanical Engineering, Beijing Institute of Technology, Beijing, China. Her research interests include intelligent control theory and decision-making methods for autonomous vehicles.



Chao Yang (M'17) received the Ph.D. degree in control science and engineering from Yanshan University, Qinhuangdao, China, in 2016. From Jun. 2012 to Dec. 2015, he was working as a joint Ph.D. student (Supervisor: Dr. Liang Li), with Department of Automotive Engineering, Tsinghua University, Beijing, China. From Jan. 2016 to Sep. 2018, he was working as a postdoctoral fellow, with the State Key Laboratory of Automotive Safety and Energy, Tsinghua University, Beijing, China. From Apr. 2017 to Apr. 2018, he was a visiting scholar at University of Victoria, Victoria, B.C., Canada. He is currently an Associate Professor with School of Mechanical Engineering, Beijing Institute of Technology, Beijing, China. Dr. Yang is currently an Associate Editor for IET Intelligent Transport Systems. His research interests include energy-efficient control for hybrid electric vehicles, advanced control theory and application on intelligent hybrid vehicles, and nonlinear control for hybrid powertrain.



Wenjie Liu received the B.S. degree from Fuzhou University, China, in 2018. She is currently working toward the M.S. degree with the School of Mechanical Engineering, Beijing Institute of Technology, Beijing, China. Her research interests include intelligent control theory, and decision-making methods for autonomous vehicles.



Changle Xiang received the Ph.D. degree from Beijing Institute of Technology, Beijing, China, in 2002. He is a currently a Professor in Beijing Institute of Technology. He is the Vice President of Beijing Institute of Technology. His research interests include vehicle dynamics and control, transmission control, and autonomous vehicle control. He has been elected to the academicians of Chinese Academy of Engineering since 2019. He is also the Director of National Key Lab of Autonomous Vehicle Platform and National Key Lab of Vehicle Transmission.



Kun Huang received his B.S. in vehicle engineering from Harbin Institute of Technology, Harbin, Heilongjiang Province, in 2012, and the Ph.D. degree in vehicle engineering from Beijing Institute of Technology, Beijing, China, in 2018. He is elected to Henan Young Postdoctoral Innovative Talents in 2019. He is currently a director engineer and a postdoctoral fellow in Zhengzhou Yutong Bus Co., LTD, His research interests include dynamics, optimal control, intelligent control of hybrid vehicles and powertrain control.